

Numerical Solution of the Burgers Equation With Neumann Boundary Noise

Bakhtiyar Ghayebi, Seyed Mohammad Hosseini, Dirk Blömker

Angaben zur Veröffentlichung / Publication details:

Ghayebi, Bakhtiyar, Seyed Mohammad Hosseini, and Dirk Blömker. 2015.
“Numerical Solution of the Burgers Equation With Neumann Boundary Noise.”
Augsburg: Universität Augsburg.

Nutzungsbedingungen / Terms of use:

licgercopyright

Dieses Dokument wird unter folgenden Bedingungen zur Verfügung gestellt: / This document is made available under the following conditions:

Deutsches Urheberrecht

Weitere Informationen finden Sie unter: / For more information see:

<https://www.uni-augsburg.de/de/organisation/bibliothek/publizieren-zitieren-archivieren/publizieren>





Universität Augsburg

Institut für
Mathematik

Bakhtiyar Ghayebi, Seyed Mohammad Hosseini, Dirk Blömker

**Numerical Solution of the Burgers Equation With Neumann
Boundary Noise**

Preprint Nr. 01/2015 — 19. Januar 2015

Institut für Mathematik, Universitätsstraße, D-86135 Augsburg

<http://www.math.uni-augsburg.de/>

Impressum:

Herausgeber:

Institut für Mathematik

Universität Augsburg

86135 Augsburg

<http://www.math.uni-augsburg.de/de/forschung/preprints.html>

ViSdP:

Dirk Blömker

Institut für Mathematik

Universität Augsburg

86135 Augsburg

Preprint: Sämtliche Rechte verbleiben den Autoren © 2015

Numerical Solution of the Burgers equation with Neumann boundary noise

B. Ghayebi* S. Mohammad Hosseini † D. Blömker ‡

December 28, 2014

Abstract

In this paper we investigate the numerical solution of the one-dimensional Burgers equation with Neumann boundary noise. For the discretization scheme we use the Galerkin approximation in space and the exponential Euler method in time. The impact of the boundary noise on the solution is discussed in several numerical examples. Moreover, we analyze and illustrate some properties of the stochastic term and study the convergence numerically.

Keywords: Burgers equation, Boundary Neumann noise, Galerkin method, Weak approximation, Exponential Euler scheme, impact of noise.

MSC2010: 60H15, 60H35, 65C05, 65C30, 60H10

1 Introduction

Stochastic partial differential equations (SPDE) arise naturally due to environmental fluctuations subject to random influences. Under some physical circumstances the physical boundary of the problem is affected by noise. Such models may be interpreted by partial differential equations (PDEs) with random Neumann boundary conditions [2, 4, 6, 10, 12]. The first paper which studied evolution problems with boundary noise was a paper [20] by Balakrishnan. Later Sowers [10] investigated general reaction diffusion equation with Neumann type boundary noise. Da Prato and Zabczyk [4] discussed the difference between problems with Dirichlet and Neumann boundary noises, as Dirichlet noise does not lead to sufficiently regular solutions. A related work for parabolic problems with boundary noise can be referred to Brzezniak and Peszat [12]. In this paper we focus on the following Burgers equation with boundary noise in a Neumann condition:

$$\begin{cases} u_t = \nu u_{xx} - uu_x, \\ u_x(0, t) = \sigma \dot{\beta}(t), & u_x(l, t) = 0, \\ u(x, 0) = u_0(x), \end{cases} \quad (1.1) \quad \boxed{1.1}$$

Here $\sigma > 0$ denotes the noise strength and $\{\beta(t)\}_{t \geq 0}$ is white noise, given by the generalized derivative of a real valued Brownian motion $\{\beta(t)\}_{t > 0}$. Finally, $\nu > 0$ denotes the viscosity. Without loss of generality after rescaling we can assume from now on to $\nu = 1$.

*b.ghayebi@modares.ac.ir

†(hossei_m@modares.ac.ir)

‡(dirk.bloemker@math.uni-augsburg.de)

We are interested in solutions given in weak or mild sense. Let $T > 0$ and (Ω, F, P) be a probability space. Let the space-time predictable processes $u : \Omega \times [0, T] \rightarrow L^2(0, l)$ be a solution that satisfies

$$\sup_{t \in [0, T]} \left(\mathbb{E} |u(t)|_{L^2(0, l)}^2 \right) < \infty .$$

According to [4], putting $u(x, t) = v(x, t) + w(x, t)$, we rewrite (1.1) as the following two PDEs in terms of $v(x, t)$ and $w(x, t)$ satisfying first a linear SPDE

$$\begin{cases} v_t = v_{xx}, & 0 < x < l, \quad t > 0, \\ v_x(0, t) = \sigma \dot{\beta}(t), & v_x(l, t) = 0, \\ v(x, 0) = 0, \end{cases} \quad (1.2) \quad \boxed{1.2}$$

and secondly a random PDE

$$\begin{cases} w_t = w_{xx} - (v + w)(v + w)_x, & 0 < x < l, \quad t > 0, \\ w_x(0, t) = 0, & w_x(l, t) = 0, \\ w(x, 0) = u_0(x). \end{cases} \quad (1.3) \quad \boxed{1.3}$$

The solution of (1.3) can be obtained by usual deterministic methods like fixed point theorems. Moreover, it can be well approximated by PDE solvers [3]. Here we are interested in the solution of the SPDE (1.2) in the weak sense, as the derivatives of w in general will not exist. Nevertheless, it is well known, that the existence of a sufficiently regular solution to (1.2) implies the existence of a solution to (1.1). See for example [4].

This paper is organized as follows. In Section 2 we formulate the problem and obtain a series expansion of the solution given as stochastic convolution. Then we obtain the numerical method based on the mild formulation of (1.2) and (1.3). In Section 3 we give numerical examples of the Burgers equation with random Neumann boundary condition and show that the noise on the boundary extends immediately to the entire domain. In Section 4 we compute the difference between solutions with $\sigma = 0$ and $\sigma \neq 0$ using different metrics. In the last section we analyzed some properties of the stochastic term, illustrated these properties numerically and verified numerically the rate of convergence of our numerical scheme.

2 Problem formulation

Denote for $l > 0$ by $L^2(0, l)$ the standard space of square-integrable functions with the standard scalar product $(u, v)_{L^2} = \int_0^l u v dx$.

Definition 2.1. An $L^2(0, l)$ valued process $v(x, t)$ is a weak solution of (1.2) for $t \in [0, T]$, if

$$(v(t), \Psi)_{L^2} = (v_0, \Psi)_{L^2} + \int_0^t (v(s), A\Psi)_{L^2} ds + \beta(t)\Psi(0)$$

for all $t \in [0, T]$ and all smooth test functions $\Psi \in C^\infty([0, l])$ satisfying Neumann boundary conditions

$$\frac{\partial \Psi}{\partial x} = 0 \quad \text{at } x = 0 \text{ and } x = l.$$

Here $A = \partial_{xx}$ is the Laplacian operator, and $D(A)$, the domain of A , is given by the subset of the standard Sobolev-space $H^2(0, l)$ satisfying Neumann boundary conditions:

$$D(A) = \left\{ \Psi \in H^2(0, l) : \frac{\partial \Psi}{\partial x}(0) = 0, \frac{\partial \Psi}{\partial x}(l) = 0 \right\}.$$

It is well known (see e.g. [3]) that the operator A has an orthonormal basis of eigenfunctions $\{g_k\}_{k \in \mathbb{N}_0}$ in $L^2(0, l)$ with corresponding non-negative eigenvalues $\{\lambda_k\}_{k \in \mathbb{N}_0}$ of $-A$, where \mathbb{N}_0 is the set of all non-negative integers.

To be more precise, in our special problem the eigenfunctions are

$$g_0(x) = \frac{1}{\sqrt{l}}, \quad g_k(x) = \sqrt{\frac{2}{l}} \cos\left(\frac{\pi k x}{l}\right), \quad k = 1, 2, \dots,$$

and the eigenvalues are $\lambda_k = \left(\frac{k\pi}{l}\right)^2$, for $k \in \mathbb{N}_0$. Moreover, A generates an analytic semigroup $\{e^{tA}\}_{t \geq 0}$ in L^2 (see [21]). This is defined by $e^{tA}g_k = e^{-t\lambda_k}g_k$ for all $k \in \mathbb{N}$ and linear extension.

2.1 Neumann Map

We define the Neumann map \mathbb{D} for any $\gamma \in \mathbb{R}$ by the solution of

$$(1 - A)\mathbb{D}\gamma = 0, \quad \partial_x \mathbb{D}\gamma(0) = \gamma, \quad \partial_x \mathbb{D}\gamma(l) = 0.$$

It is known that $\mathbb{D} : \mathbb{R} \rightarrow H^2([0, l])$ is a continuous linear operator [11]. In fact, we have an explicit expression for this linear operator

$$\mathbb{D}(\gamma) = \frac{e^x + e^{2l}e^{-x}}{1 - e^{2l}}\gamma.$$

From [5] we immediately obtain the following theorem about the weak solution of (1.2).

Theorem 1

Theorem 2.2. *For the Neumann boundary value problem (1.2) there is a unique solution in H^α for all $\alpha < \frac{1}{2}$. Moreover, the solution is given by*

$$v(t) = (1 - A) \int_0^t e^{A(t-s)} \mathbb{D} \sigma d\beta(s).$$

Proof. see [5]. □

Below we follow [6] to provide an explicit formula for v in terms of Fourier series. For $\gamma \in \mathbb{R}$, by the definition of \mathbb{D} and using integration by parts we obtain for $g \in D(A)$

$$\begin{aligned} (\mathbb{D}\gamma, (1 - A)g)_{L^2} &= (\mathbb{D}\gamma, g)_{L^2} - \int_0^l \mathbb{D}\gamma \cdot g_{xx} dx \\ &= (\mathbb{D}\gamma, g)_{L^2} - \int_0^l (\mathbb{D}\gamma)_{xx} g dx + (\mathbb{D}\gamma)_x \cdot g|_0^l \\ &= -\gamma g(0). \end{aligned}$$

Hence,

$$\begin{aligned}
(v(t), g_k)_{L^2} &= \left(\int_0^t e^{A(t-s)} \mathbb{D} \sigma d\beta(s), (1-A)g_k \right)_{L^2} \\
&= \int_0^t e^{-(t-s)\lambda_k} (\mathbb{D} \sigma d\beta(s), (1-A)g_k)_{L^2} \\
&= \sigma g_k(0) \int_0^t e^{-(t-s)\lambda_k} d\beta(s).
\end{aligned}$$

Therefore, we obtain

$$v(t) = \sigma \sum_{k \in \mathbb{N}_0} g_k(0) \int_0^t e^{-(t-s)\lambda_k} d\beta(s) g_k.$$

Finally we have

$$v(t) = \sigma g_1(0) \sum_{k \in \mathbb{N}} \int_0^t e^{-(t-s)\lambda_k} d\beta(s) g_k + \sigma g_0^2(0) \beta(t). \quad (2.1) \quad \boxed{1.4}$$

This looks very similar to a standard stochastic convolution with space-time white noise, but the key difference is that all Brownian motions in the series are actually the same. We would obtain exactly the same stochastic convolution, in case of an additive point forcing of the type $\delta_0 d\beta$, where δ_0 is the Dirac-function on the left boundary $x = 0$.

2.1.1 The effect of Noise On Both Sides

Let us briefly remark on the effect of noise in both boundary conditions. We now consider (1.1) with the new conditions $u_x(0, t) = \sigma_1 \dot{\beta}_1(t)$, $u_x(l, t) = \sigma_2 \dot{\beta}_2(t)$. We can define the Neumann map $\hat{\mathbb{D}}$ for any $\gamma = (\gamma_1, \gamma_2) \in \mathbb{R}^2$ by the solution of

$$(1-A)\hat{\mathbb{D}}\gamma = 0, \quad \partial_x \hat{\mathbb{D}}\gamma_1(0) = \gamma_1, \quad \partial_x \hat{\mathbb{D}}\gamma_2(l) = \gamma_2.$$

We then have an explicit expression for this linear operator as

$$\hat{\mathbb{D}}(\gamma) = \frac{e^x + e^{2l}e^{-x}}{1 - e^{2l}} \gamma_1 + \frac{e^x + e^{-x}}{e^l - e^{-l}} \gamma_2.$$

Then with a similar proof as before we obtain $v(t)$ for these new conditions as follows:

$$\begin{aligned}
v(t) &= \sigma_1 g_1(0) \sum_{k \in \mathbb{N}} \int_0^t e^{-(t-s)\lambda_k} d\beta_1(s) g_k + \sigma g_0^2(0) \beta_1(t) \\
&\quad + \sigma_2 \sum_{k \in \mathbb{N}} (-1)^k g_k(1) \int_0^t e^{-(t-s)\lambda_k} d\beta_2(s) g_k + \sigma_2 g_0^2(1) \beta_2(t).
\end{aligned} \quad (2.2)$$

Note that we can easily check that $\mathbb{E}\|v(t)\|_{H^\alpha}^2 < \infty$, if and only if $\sum_{k=0}^{\infty} \lambda_k^{1-\alpha} < \infty$, which in turn is true, if and only if $\alpha < \frac{1}{2}$.

The structure of the noise influence is very similar, and therefore in the sequel for simplicity we will only consider (1.1) with noise only in one of the boundary condition:

$$u_x(0, t) = \sigma \dot{\beta}(t), \quad u_x(l, t) = 0.$$

2.2 Mild Formulation

Now we turn to the non-linear equation. The mild solution of the random PDE (1.3) is given by

$$w(t) = e^{tA}u_0 + \int_0^t e^{A(t-s)} \left(-\frac{1}{2} \frac{\partial}{\partial x} (v(s) + w(s))^2 \right) ds, \quad \text{for } t > 0.$$

This is equivalent to the fact that the mild solution of (1.1) exists, see Theorem 2.3, and is given by

$$u(t) = e^{tA}u_0 + \int_0^t e^{A(t-s)} \left(-\frac{1}{2} \frac{\partial}{\partial x} u^2(s) \right) ds + v(t).$$

Theorem2

Theorem 2.3. *Suppose for the Ornstein-Uhlenbeck processes $v \in C^0([0, T], L^2)$, and define $F(u) = -\frac{1}{2} \frac{\partial}{\partial x} u^2$. Then for every $u_0 \in L^2$ there exists $u \in C^0([0, T], L^2)$ which satisfies*

$$u(t) = e^{tA}u_0 + \int_0^t e^{A(t-s)} F(u(s)) ds + v(t).$$

Proof. This is standard. See for example [2]. It is sufficient that a F is a locally Lipschitz continuous mapping from L^2 to some $H^{-\alpha}$ for some $\alpha \in (3/2, 2)$. Moreover, standard a-priori estimates for w in L^2 hold. \square

2.3 Numerical scheme

For simplicity of presentation suppose in the following $l = 1$. Nevertheless, this is not a severe restriction, as we can rescale the domain by a factor $1/l$, and time by $1/l^2$, which just results in a small ν and a changed noise strength.

Similar as the numerical scheme in [23], which is based on the work of Jentzen and Kloeden [7, 8] we consider the exponential Euler method for the Galerkin approximation of the mild solution of the Burgers equation (1.1). Recall the mild solution

$$u(t) = e^{tA}u(0) + \int_0^t e^{A(t-s)} F(u(s)) ds + (1 - A) \int_0^t e^{A(t-s)} D\sigma d\beta(s), \quad (2.3) \quad 1.5$$

where we have defined

$$F(u) = -\frac{1}{2} \frac{\partial}{\partial x} (u^2).$$

Projecting equation (2.3) onto the subspace X of $L^2(0, l)$, spanned by the first $N + 1$ -eigenfunctions

$$\{g_0(x), g_1(x), \dots, g_N(x)\},$$

the Galerkin approximation with $N + 1$ degrees of freedom in $L^2(0, 1)$ is given by

$$u^N(t) = \sum_{n=0}^N u_n(t) g_n,$$

and additionally for the nonlinearity we approximate

$$F^{(N)}(u^N(t)) = \sum_{n=0}^N F_n(u^N(t)) g_n,$$

where

$$u_n(t) = (u^N(t), g_n)_{L^2}, \quad F_n(u^N) = (F(u^N), g_n)_{L^2}, \quad n = 0, 1, \dots, N.$$

From Equations (2.3) and (2.1), we obtain the Galerkin approximation in terms of the following stochastic differential equation (SDE) in \mathbb{R}^{N+1} of the form,

$$u_n(t) = e^{-t\lambda_n} u_n(0) + \int_0^t e^{-\lambda_n(t-s)} F_n(u^N(s)) ds + \sigma g_n(0) \int_0^t e^{-(t-s)\lambda_n} d\beta(s). \quad (2.4) \quad \boxed{\text{Galerkin}}$$

Thus for a fixed small time $\Delta t > 0$ we obtain

$$\begin{aligned} u_n(t + \Delta t) &= e^{-\Delta t \lambda_n} u_n(t) + \int_0^{\Delta t} e^{-\lambda_n(\Delta t-s)} F_n(u^N(t+s)) ds \\ &\quad + \sigma g_n(0) \int_0^{\Delta t} e^{-(\Delta t-s)\lambda_n} d\beta(t+s). \end{aligned}$$

Applying an exponential Euler-scheme yields

$$u_n(t + \Delta t) \approx e^{-\lambda_n \Delta t} u_n(t) + \frac{1 - e^{-\lambda_n \Delta t}}{\lambda_n} F_n(u^N(t)) + \left(\frac{1}{\lambda_n} (1 - e^{-2\lambda_n \Delta t}) \right)^{\frac{1}{2}} \sigma R_n \quad (2.5) \quad \boxed{1.6}$$

for $n = 1, 2, \dots, N$, and for $n = 0$

$$u_0(t + \Delta t) = u_0(t) + F_0(u^N(t)) \Delta t + \sqrt{\Delta t} \sigma R_0, \quad (2.6) \quad \boxed{1.7}$$

where the normal random variables R_n depend all on the same Brownian motion. Finally, we can define the full numerical scheme

$$u_{n,k+1} = e^{-\lambda_n \Delta t} u_{n,k} + \frac{1 - e^{-\lambda_n \Delta t}}{\lambda_n} F_n(u_k^N) + \left(\frac{1}{\lambda_n} (1 - e^{-2\lambda_n \Delta t}) \right)^{\frac{1}{2}} \sigma R_{n,k} \quad (2.7) \quad \boxed{1.8}$$

for $n = 1, 2, \dots, N$, and

$$u_{0,k+1} = u_{0,k} + F_0(u_k^N) \Delta t + \sqrt{\Delta t} \sigma R_{0,k} \quad (2.8) \quad \boxed{1.9}$$

where for fixed n the family $\{R_{n,k}\}_{k=0,1,\dots}$ consists of independent standard normally distributed random variables, which we discuss in more detail how they can be generated efficiently in the next section. Once we get all u_n , we obtain the approximate solution

$$u^N(x, t) = \sum_{n=0}^N u_n(t) g_n(x).$$

3 Numerical simulations

In this section as an example we suppose $u_0(x) = \frac{6}{5} \cos(\pi x)$ and use (2.6) and (2.7) to solve the problem (1.1). See Figures 1 and 2. There is nothing special about the initial condition and other choices would yield similar results.

Note that the $R_{n,k}$ are highly dependent on each other for fixed k . Let for fixed $t \geq 0$ $\beta^{(t)}$ be a standard Brownian motion defined by $\beta^{(t)}(s) = \beta(t+s) - \beta(t)$. Consider

$$X_n = \int_0^{\Delta t} e^{-(\Delta t-s)\lambda_n} d\beta^{(t)}(s) = \left(\frac{1}{2\lambda_n} (1 - e^{-2\lambda_n \Delta t}) \right)^{\frac{1}{2}} R_n$$

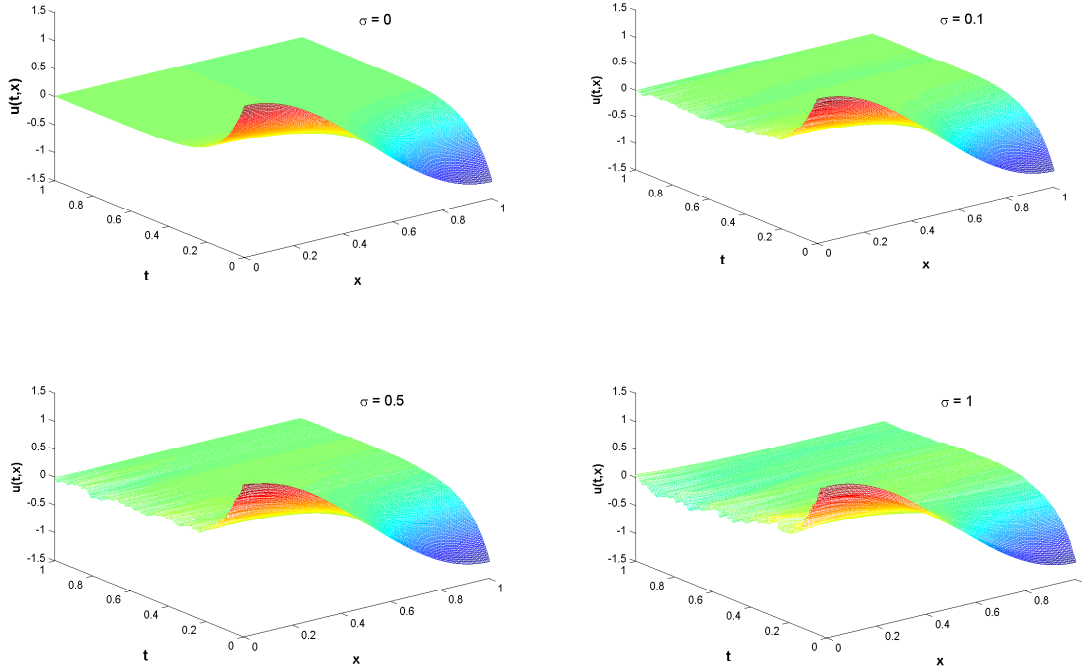


Figure 1: Solution of Burgers equation with Neumann boundary noise, for noise intensities: $\sigma = 0, 0.1, 0.5, 1$ and with $u_0(x) = \frac{6}{5}\cos(\pi x)$, $N = 200$, $\Delta t = 1/300$, $\nu = 1$.

fig1

then obviously

$$\mathbb{E}X_n X_m = \int_0^{\Delta t} e^{-(\Delta t-s)\lambda_n} e^{-(\Delta t-s)\lambda_m} ds = \frac{1}{\lambda_n + \lambda_m} (1 - e^{-\Delta t(\lambda_n + \lambda_m)}) \neq 0.$$

Therefore, for generating X_n , let Σ be the covariance matrix of X , which is an $n \times n$ matrix in which the $(i, j)^{th}$ element is given by $\Sigma_{i,j} := Cov(X_i, X_j)$. Our aim at this step is to generate $X = (X_1, X_2, \dots, X_n)$ where $X \sim MN(0, \Sigma)$. Obviously, when $Z_i \sim N(0, 1)$ and iid for $i = 1, 2, \dots, n$, we can obtain:

$$l_1 Z_1 + l_2 Z_2 + \dots + l_n Z_n \sim N(0, \sigma^2)$$

where $\sigma^2 := l_1^2 + l_2^2 + \dots + l_n^2$. That is, a linear combination of independent normal random variables is again normal.

More generally, let L be an $n \times m$ matrix and let $\mathbf{Z} = (Z_1, Z_2, \dots, Z_n) \sim MN(0, I_n)$ where I_n is the $n \times n$ identity matrix, then $L^T \mathbf{Z} \sim MN(0, L^T L)$. Hence, our problem clearly reduces to finding L such that $L^T L = \Sigma$. We can find such a matrix, L , using the Cholesky decomposition of Σ .

Hence, we have mentioned above, for any k , $R_{n,k}$ can be generated. Then with these random numbers we have applied our numerical method to the problem (1.1) with $u_0(x) = \frac{6}{5}\cos(\pi x)$. Note that for comparing the solutions with different N pathwise, we first calculate the X_i for some large N and then use them for all smaller N . The results for $\nu = 1$ and some various intensities are shown in Figure 1. The plots in this Figure illustrate that

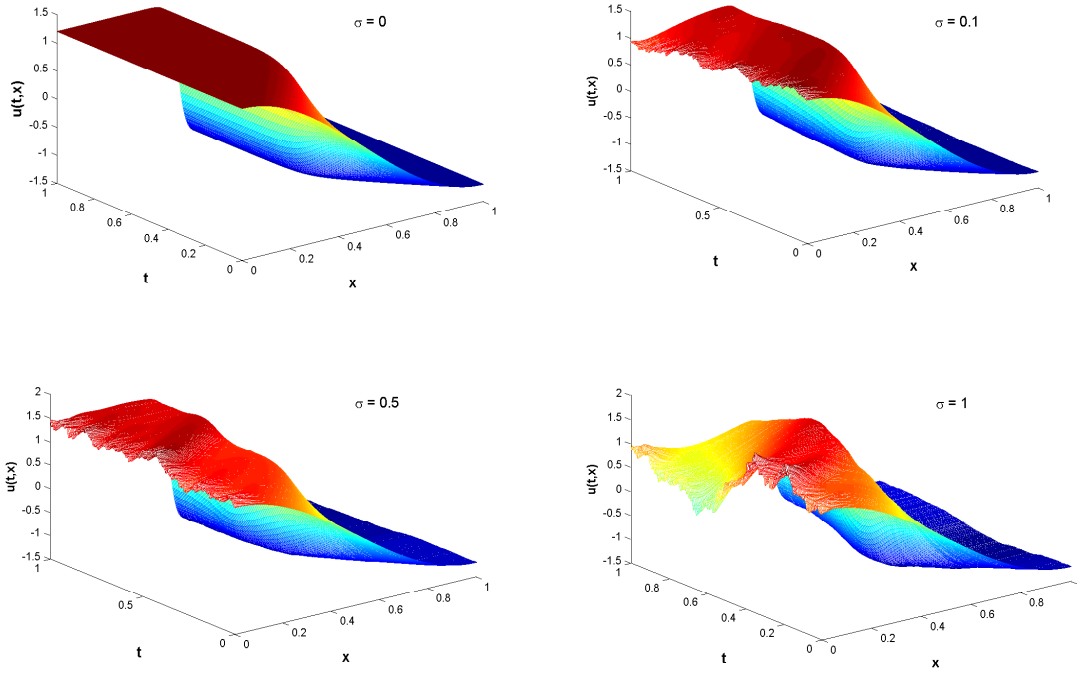


Figure 2: Solution of Burgers equation with Neumann boundary noise, for noise intensities: $\sigma = 0, 0.1, 0.5, 1$ and with $u_0(x) = \frac{6}{5} \cos(\pi x)$, $N = 200$, $\Delta t = 1/300$, $\nu = 1/50$. Recall that small ν corresponds to slow time and large domains. The noise has significantly less impact at $x = 1$.

fig2

as the noise intensity σ grows, the corresponding solution undulates more and more and spreads all over the domain.

Small ν means large domains and slow times. So for a more illustration of the impact of noise, we also increase the amount of noise by adding a small constant $\nu = 1/50$ in front of the u_{xx} in (1.1), see Figure 2. This figure confirms that by increasing the effect of noise the solution goes to 0 much slower. Further investigation on the impact of the noise on the solution will also be carried out in Section 4.

4 The impact of boundary noise on the solution

In order to quantify the impact of noise on the solution of the Burgers equation with Neumann boundary condition, we compute the difference between solutions corresponding to $\sigma = 0$ and $\sigma \neq 0$ using different metrics [10, 13].

For the impact of noise to be observed better by increasing the amount of noise, the initial condition $u_0(x) = 0$ is used for which obviously the deterministic solution corresponding to $\sigma = 0$ is explicitly 0 for all times.

We then compute the root mean square difference (RMSD) between the numerical solutions of equation without noise ($\sigma = 0$) and with the Neumann boundary noise ($\sigma \neq 0$) similar as [22], with the following three metrics. Recall that $u_{\sigma=0}(x, t) = 0$, as we have

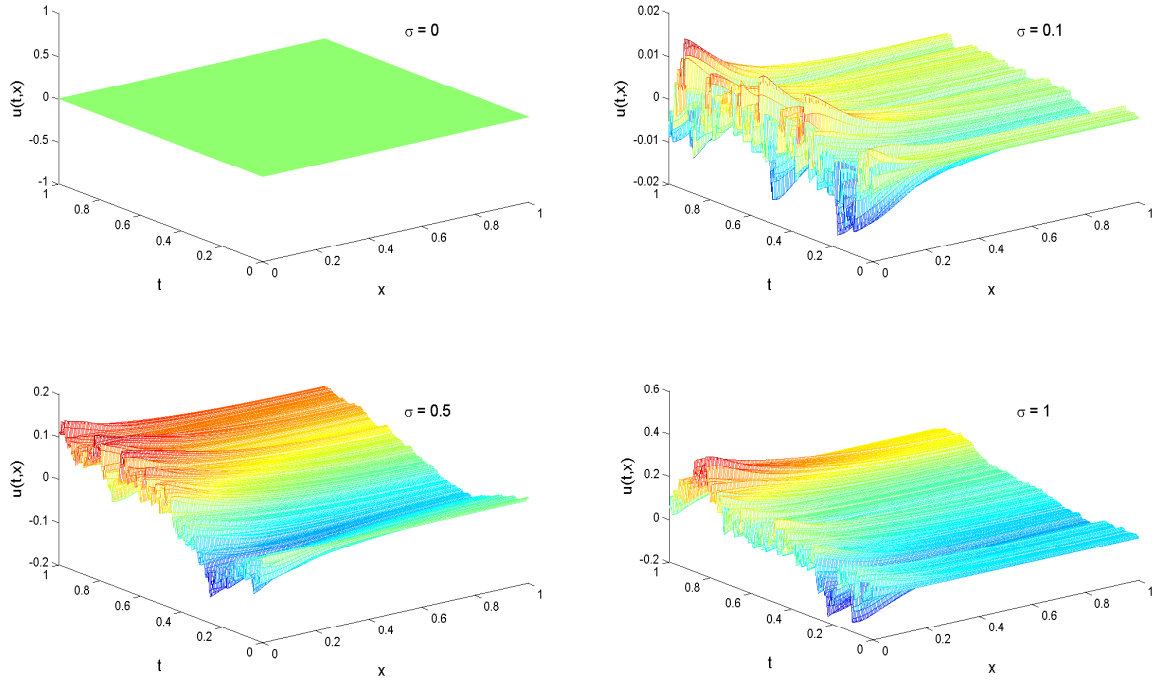


Figure 3: Solution of Burgers equation with Neumann boundary noise, for noise intensities: $\sigma = 0, 0.1, 0.5, 1$ and with $u_0(x) = 0, N = 200, \Delta t = 1/300, \nu = 1$. The noise spreads immediately through the whole domain, but it seems that the main impact is on the constant Fourier-mode.

fig3

chosen here $u(0) = 0$.

Definition 4.1. We define

1. $RMSD_1(x, t) = \sqrt{\mathbf{E}|u_{\sigma \neq 0}(x, t) - u_{\sigma=0}(x, t)|^2}$
2. $RMSD_2(x) = \sqrt{\mathbf{E} \int_0^1 |u_{\sigma \neq 0}(x, t) - u_{\sigma=0}(x, t)|^2 dt}$
3. $RMSD_3(t) = \sqrt{\mathbf{E} \int_0^1 |u_{\sigma \neq 0}(x, t) - u_{\sigma=0}(x, t)|^2 dx}$

The plots in Figure 3 illustrate the impact of increasing noise very clearly, showing that the noise on the boundary grows immediately into the entire domain (30 realizations have been used to calculate the mean). Also, it is observed, see Figures 4-6, that with $\sigma = 0.01$ the noise on the boundary $x = 0$ spreads at once to the interior domain ($0 < x < 1$). In addition, in Figure 7 we have illustrated $\sqrt{\mathbf{E} \left| u_{\sigma \neq 0}(x, t) - \int_0^1 u_{\sigma \neq 0}(x, t) dx \right|^2}$ for $\sigma = 0.01$. In comparison with Figure 3 the the impact of the noise on the other non-constant modes is significantly smaller, but still the noise spreads immediately through the whole domain.

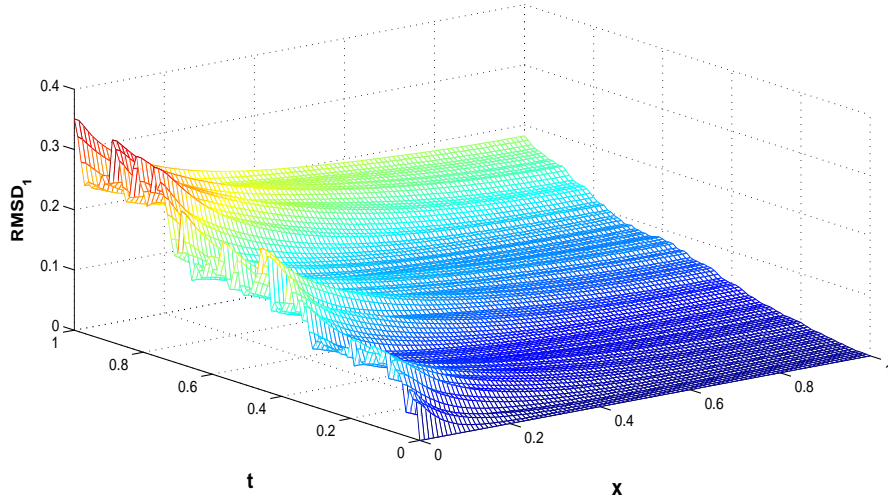


Figure 4: Root mean square difference ($RMSD_1$) of the Burgers equation with random Neumann boundary noise, with respect to time and space, for $\sigma = 0.01$, with $u_0(x) = 0$.

fig4

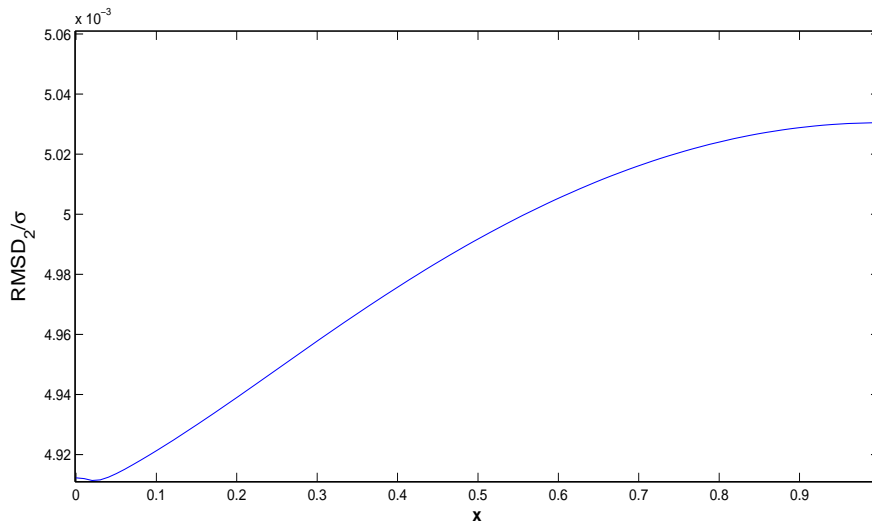


Figure 5: Root mean square difference ($RMSD_2$)/ σ of the Burgers equation with random Neumann boundary noise, with respect to space, for $\sigma = 0.01$, with $u_0(x) = 0$. The impact of noise decays from the noise source $x = 0$ to $x = 1$.

fig5

5 Analysis of $v(t)$

In this section firstly we calculate $E|v(t, x)|^2$ and then show that $v(t, 0)$ is unbounded. This shows that numerical analysis in L^∞ -norm is not possible. For this from (2.1) we have

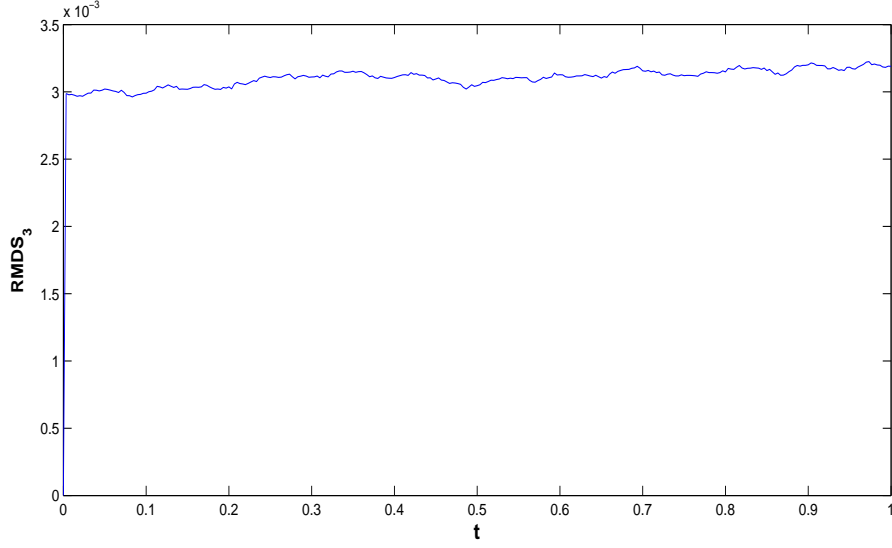


Figure 6: Root mean square difference ($RMSD_3$) of the Burgers equation with random Neumann boundary noise, with respect to time, for $\sigma = 0.01$, with $u_0(x) = 0$. At each point of time the average impact of noise is roughly the same.

fig6

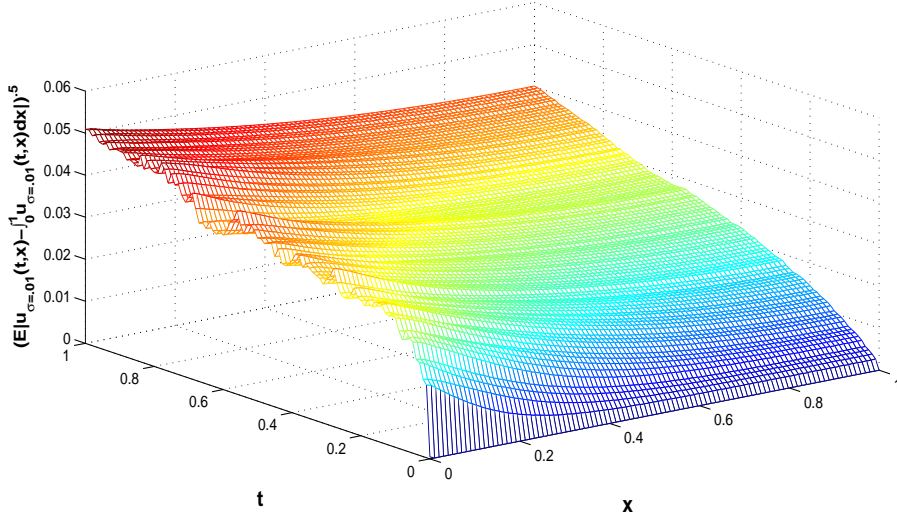


Figure 7: $\sqrt{\mathbb{E} \left| u_{\sigma \neq 0}(x, t) - \int_0^1 u_{\sigma \neq 0}(x, t) dx \right|^2}$ of the Burgers equation with random Neumann boundary noise, with respect to time and space, for $\sigma = 0.01$, with $u_0(x) = 0$.

fig7

$$\begin{aligned} \mathbb{E}|v(t, x)|^2 &= \mathbb{E} \left(\sigma g_1(0) \sum_{k=1}^{\infty} \int_0^t e^{-(t-s)\lambda_k} d\beta_s g_k(x) + \sigma g_0^2(0) \beta(t) \right)^2 \\ &= \mathbb{E} \left(\left(\sigma g_1(0) \sum_{k=1}^{\infty} \int_0^t e^{-(t-s)\lambda_k} d\beta_s g_k(x) \right)^2 \right) \end{aligned}$$

$$\begin{aligned}
& + 2\sigma^2 g_1(0)g_0^2(0)\beta(t) \sum_{k=1}^{\infty} \int_0^t e^{-(t-s)\lambda_k} d\beta_s g_k(x) + (\sigma g_0^2(0)\beta(t))^2 \Big) \quad (5.1) \quad \boxed{1.10} \\
& = \mathbb{E} \left(\sigma g_1(0) \sum_{k=1}^{\infty} \int_0^t e^{-(t-s)\lambda_k} d\beta_s g_k(x) \right)^2 \\
& \quad + \mathbb{E} \left(2\sigma^2 g_1^3(0)\beta(t) \sum_{k=1}^{\infty} \int_0^t e^{-(t-s)\lambda_k} d\beta_s g_k(x) \right) + \mathbb{E} \left(\sigma g_0^2(0)\beta(t) \right)^2
\end{aligned}$$

Using the Itô isometry we obtain

$$\begin{aligned}
\mathbb{E}|v(t, x)|^2 & = \sigma^2 g_1^2(0) \sum_{k=1}^{\infty} \sum_{l=1}^{\infty} \left(\frac{(1 - e^{-t(\lambda_k + \lambda_l)}) g_k(x) g_l(x)}{\lambda_k + \lambda_l} \right) \quad (5.2) \quad \boxed{1.12} \\
& \quad + 2\sigma^2 g_1(0)g_0^2(0) \sum_{k=1}^{\infty} \frac{(1 - e^{-t\lambda_k}) g_k(x)}{\lambda_k} + \sigma^2 g_0^4(0)t
\end{aligned}$$

Now we substitute $\lambda_k, \lambda_l, g_k$ and g_l , therefore we have

$$\begin{aligned}
\mathbb{E}|v(t, x)|^2 & = \frac{2\sigma^2}{\pi^2} \sum_{k=1}^{\infty} \sum_{l=1}^{\infty} \left(\frac{(1 - e^{-t\pi^2(k^2+l^2)}) \cos(kx) \cos(lx)}{k^2 + l^2} \right) \quad (5.3) \quad \boxed{1.13} \\
& \quad + \frac{2\sqrt{2}\sigma^2}{\pi^2} \sum_{k=1}^{\infty} \frac{(1 - e^{-t\pi^2 k^2}) \cos(kx)}{k^2} + \sigma^2 t.
\end{aligned}$$

Now let $x = 0$ in [\(5.1\)](#). Then,

$$\mathbb{E}|v(t, 0)|^2 = \mathbb{E} \left| \int_0^t \left(\sigma g_1(0) \sum_{k=1}^{\infty} e^{-\pi^2(t-s)k^2} g_k(0) + \sigma g_0^2(0) \right) d\beta_s \right|^2. \quad (5.4) \quad \boxed{1.14}$$

From Itô isometry we obtain

$$\begin{aligned}
\mathbb{E}|v(t, 0)|^2 & = \int_0^t \left(\sigma g_1(0) \sum_{k=1}^{\infty} e^{-\pi^2(t-s)k^2} g_k(0) + \sigma g_0^2(0) \right)^2 ds \\
& \geq C \int_0^t \left(\int_1^{\infty} e^{-\pi^2(t-s)x^2} dx \right)^2 ds
\end{aligned}$$

where C depends on σ and $g_k(0)$. Now let $I = \int_1^{\infty} e^{-\pi^2(t-s)x^2} dx = \int_1^{\infty} e^{-\pi^2(t-s)y^2} dy$. Then we have

$$I^2 = \int_1^{\infty} \int_1^{\infty} e^{-\pi^2(t-s)(x^2+y^2)} dx dy.$$

With use of polar coordinates

$$I^2 = \int_0^{\frac{\pi}{2}} \int_{\sqrt{2}}^{\infty} e^{-\pi^2(t-s)r^2} r dr d\theta = \frac{e^{-2\pi^2(t-s)}}{2\pi^2(t-s)}.$$

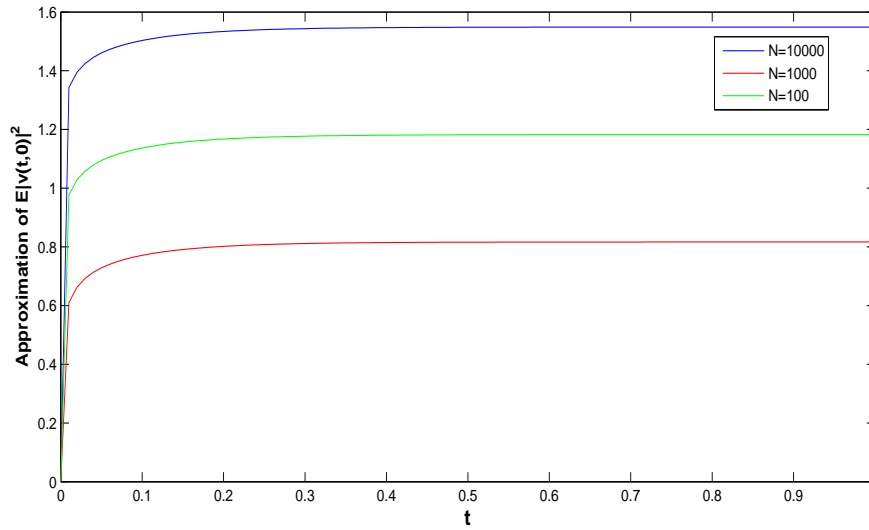


Figure 8: Approximation of $E|v(t,0)|^2$ with respect to time, sum of first N terms of right-hand of (5.3) for $N = 100, 1000$, and 10000 , confirming unboundedness of $E|v(t,0)|^2$. We see a logarithmic divergence.

fig9

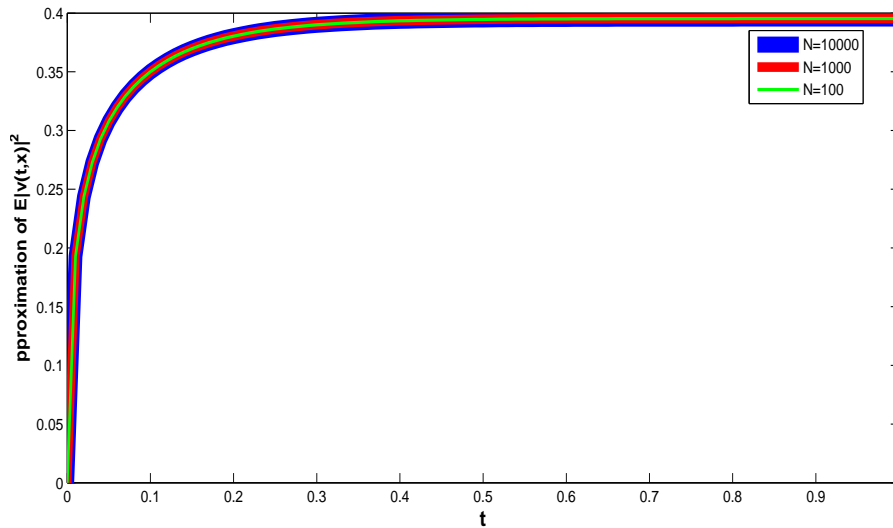


Figure 9: Approximation of $E|v(t,x)|^2$ with respect to time and $x = .1$, sum of first N terms of right-hand of (5.3) for $N = 100, 1000$, and 10000 , confirming boundedness of $E|v(t,x)|^2$ in $x = .1$. It seems to converge even very fast with increasing number of Galerkin-Modes.

fig10

Therefore

$$E|v(t, 0)|^2 \geq C \int_0^t \frac{e^{-2\pi^2(t-s)}}{2\pi^2(t-s)} ds = C \frac{1}{2\pi^2} \int_0^t \frac{e^{-2\pi^2 s}}{s} ds = \infty$$

hence $E|v(t, 0)|^2 = \infty$. Therefore we have shown that the stochastic convolution v is not bounded at 0, because of lack regularity we can not expect uniform bounds on the solution.

For more illustrative properties we plotted the approximation of $E|v(t, x)|^2$ for $x = 0$, $x = 0.1$ and $x = 1$ in Figure 8, according to Figure 8 we see that $E|v(t, 0)|^2$ is divergent and $E|v(t, x)|^2$ for $x \neq 0$ is convergent, see Figure 9. The divergence is logarithmic, as expected.

In addition we plotted in Figures 10-12 the Monte-Carlo approximation of $E|v(t, x)|^2$ with respect to time and $x = 1$ from (5.3) and also $E|u(t, x)|^2$ for $N = 200$ and 300 , in which only 50 realizations have been used to calculate the mean. Even with a few modes and very few realizations, the divergence is already obvious.

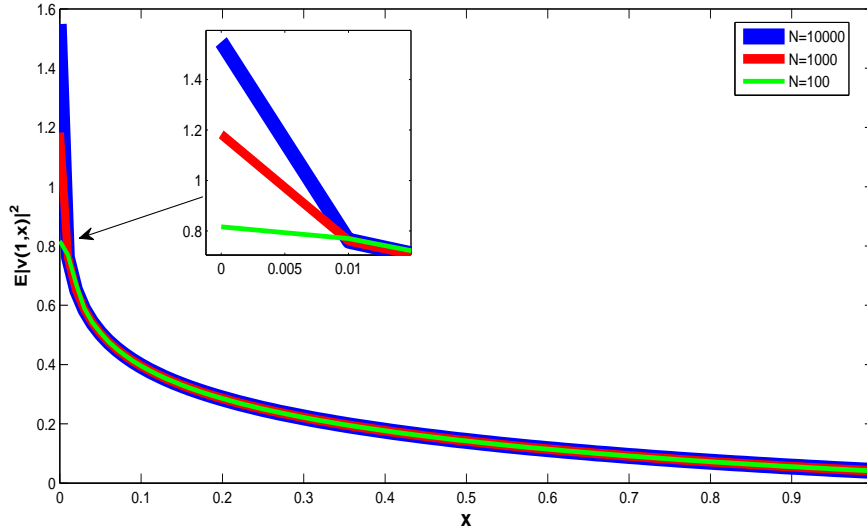


Figure 10: Approximation of $E|v(t, x)|^2$ with respect to space and $t = 1$, sum of first N terms of right-hand of (5.3) for $N = 100, 1000$, and 10000 , confirming unboundedness of $E|v(t, x)|^2$ for $x = 0$ and its boundedness for $x \neq 0$.

fig11

Now to know more about the properties of the stochastic function $v(t)$, in the lines of [6] we also try to show the properties of the stochastic function $v(t)$. We will compare $v(t)$ by a suitable Wiener process $W(t)$ driving the SPDE in (5.6) that the property of which is known. We have to set relation between $v(t)$ and a Wiener process $W(t)$ which obtained as follows:

$$Z(t) = \alpha \sum_{k \in \mathbb{N}} \int_0^t e^{-(t-s)\lambda_k} d\beta_k(s) g_k + \alpha \beta_0(t). \quad (5.5) \quad 1.15$$

In fact $Z(t)$ is nothing other than the stochastic term of mild solution of the below equation:

$$\begin{cases} z_t = z_{xx} - \alpha W_t, \\ z_x(\cdot, 0) = 0 \quad z_x(\cdot, 1) = 0. \end{cases} \quad (5.6) \quad 1.16$$

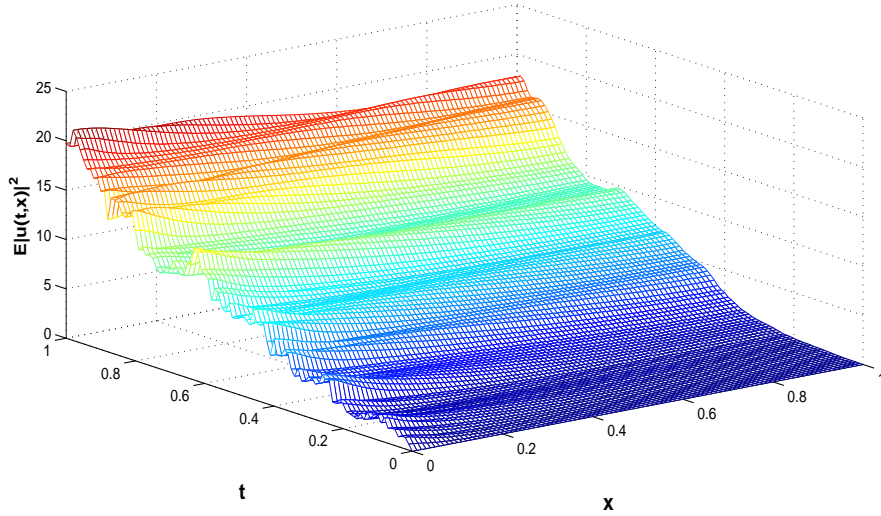


Figure 11: Approximation of $E|u(t, x)|^2$ with respect to time and space, for $N = 100$.

12

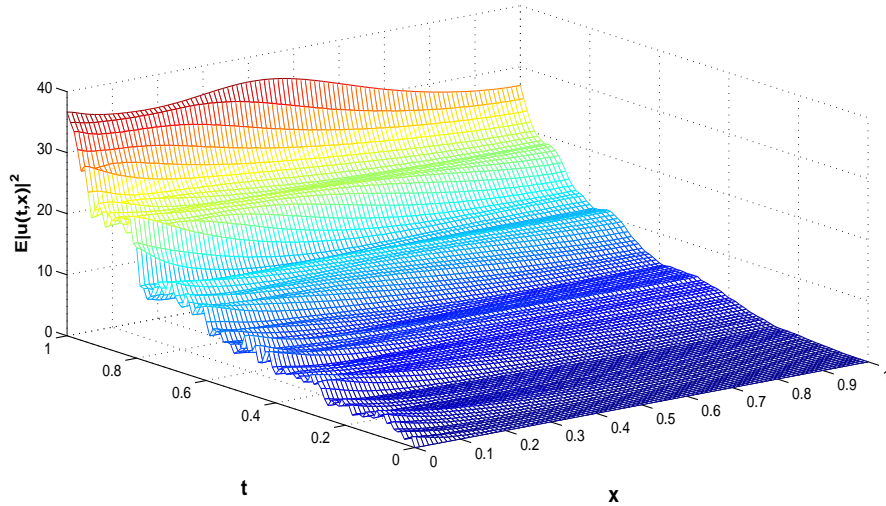


Figure 12: Approximation of $E|u(t, x)|^2$ with respect to time and space, for $N = 200$. This is for $x > 0$ very similar to Figure 11 with $N = 100$, but for $x = 0$ the values are much bigger.

fig13

Note that the difference between $Z(t)$ in (5.5) and $v(t)$ in (2.1) is that the Brownian motions used in $v(t)$ are actually the same, but in $W(t)$ independent Brownian motions are used. Since properties of $Z(t)$ are known to us, we try to introduce the following criteria to find relation between $Z(t)$ and $v(t)$. This is just the same approach of [6]. The first criterion that will be used is the mean energy M_u such as:

$$M_u = \int_0^1 E[u(t, x) - \bar{u}(t)]^2 dx \quad (5.7)$$

1.17

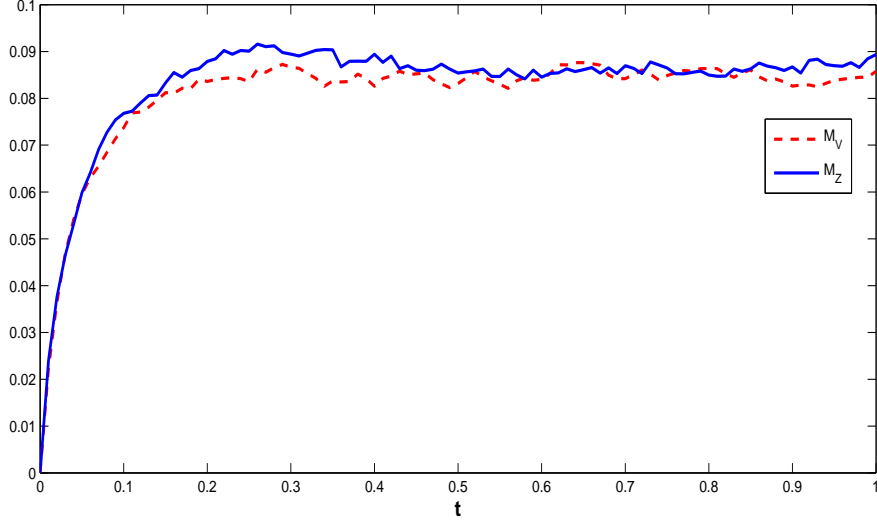


Figure 13: Numerical estimate of the mean energy M_V and M_Z to illustrate the results of Theorem 5.1. Already very few realizations in the Monte-Carlo simulation yields very good agreement of the curves. fig14

where

$$\bar{u}(t) = \int_0^1 u(t, x) dx.$$

The second one will be the averaged mean correlation function \hat{C} as:

$$\hat{C}(t, r) = \frac{1}{2} [C(t, r) + C(t, -r)] \quad (5.8) \quad 1.18$$

where

$$C(t, r) = \int_0^1 \mathbb{E} [u(t, x) - \bar{u}(t)] [u(t, x+r) - \bar{u}(t)] dx. \quad (5.9) \quad 1.19$$

Note that $C(t, r)$ can be defined for any $r \in \mathbb{R}$. For the above mentioned criteria we can state the following Theorem.

Theorem3

Theorem 5.1. *Suppose $\alpha = \sigma g_1(0)$ then we have*

$$M_v = M_Z.$$

Before proving the theorem, we calculate M_V and M_Z numerically (by setting the nonlinear term 0 in (1.1) and $u_0 = 0$) and plot them in Figure 13, the performance confirms the result of Theorem 5.1. Even under discretization and using not that many realizations, the estimated curves for the mean values agree well. fig14

Proof. First due to $\bar{v}(t) = \sigma g_0^2(0)\beta(t)$ we obtain

$$v(t, x) - \bar{v}(t) = \sigma g_1(0) \sum_{k=1}^{\infty} \int_0^t e^{-(t-s)\lambda_k} d\beta(s) g_k(x). \quad (5.10) \quad \text{e:key}$$

We have

$$M_v = \mathbb{E} \int_0^1 [v(t, x) - \bar{v}(t)]^2 dx = \mathbb{E} \int_0^1 \left(\sigma g_1(0) \sum_{k=1}^{\infty} \int_0^1 e^{-(t-s)\lambda_k} d\beta(s) g_k(x) \right)^2 dx. \quad (5.11) \quad 1.20$$

Therefore using $\int_0^1 g_k(x) g_l(x) dx = 0$ for $k \neq l$ and Itô isometry we obtain:

$$M_v = \sigma^2 g_1^2(0) \sum_{k=1}^{\infty} \int_0^t e^{-2s\lambda_k} ds. \quad (5.12) \quad 1.21$$

Similarly we have

$$M_Z = \mathbb{E} \int_0^1 \left(\alpha \sum_{k=1}^{\infty} \int_0^1 e^{-(t-s)\lambda_k} d\beta_k(s) g_k(x) \right)^2 dx = \alpha^2 \sum_{k=1}^{\infty} \int_0^t e^{-2s\lambda_k} ds. \quad (5.13) \quad 1.22$$

Therefore from (5.12) and (5.13) we obtain the claim of the theorem. \square

According to the Theorem above, we see that they have a different structure but have the same mean energy. Nevertheless single trajectories will behave quite differently.

In the following theorem, we show that the averaged mean correlation of $v(t)$ and $Z(t)$ is also the same.

Theorem4

Theorem 5.2. *Suppose $\alpha = \sigma g_1(0)$ then*

$$\hat{C}_v(t, r) = \hat{C}_Z(t, r).$$

Proof. First note that

$$\begin{aligned} g_k(x) g_m(x+r) &= g_k(0) g_m(0) \cos(\pi k x) \cos(\pi m(x+r)) \\ &= \frac{1}{2} g_k(0) g_m(0) (\cos(\pi(k-m)x - \pi m r) + \cos(\pi(k+m)x + \pi m r)) \end{aligned}$$

Thus using for $\ell \neq 0$ we have $\int_0^1 \cos(\pi \ell x + b) dx = \int_0^1 \cos(\pi \ell x) dx$ due to periodicity, we obtain

$$\int_0^1 g_k(x) g_m(x+r) dx = \begin{cases} 0 & : k \neq m \\ g_k^2(0) \cos(\pi r k) & : k = m \end{cases}$$

Hence from (5.10) using Itô-isometry

$$\begin{aligned} C_v(t, r) &= \int_0^1 \mathbb{E} [v(t, x) - \bar{v}(t)] [v(t, x+r) - \bar{v}(t)] dx \\ &= \sigma^2 g_1^2(0) \sum_{k=1}^{\infty} \int_0^t e^{-2(t-s)\lambda_k} ds g_k^2(0) \cos(\pi r k). \end{aligned} \quad (5.14) \quad 1.24$$

On the other hand, similar as above, we obtain,

$$\begin{aligned} C_Z(t, r) &= \int_0^1 \mathbb{E} [Z(t, x) - \bar{Z}(t)] [Z(t, x+r) - \bar{Z}(t)] dx \\ &= \alpha^2 \sum_{k=1}^{\infty} \int_0^t e^{-2(t-s)\lambda_k} ds g_k^2(0) \cos(\pi r k) \end{aligned} \quad (5.15) \quad 1.26$$

From (5.14) and (5.15) the claim follows. \square

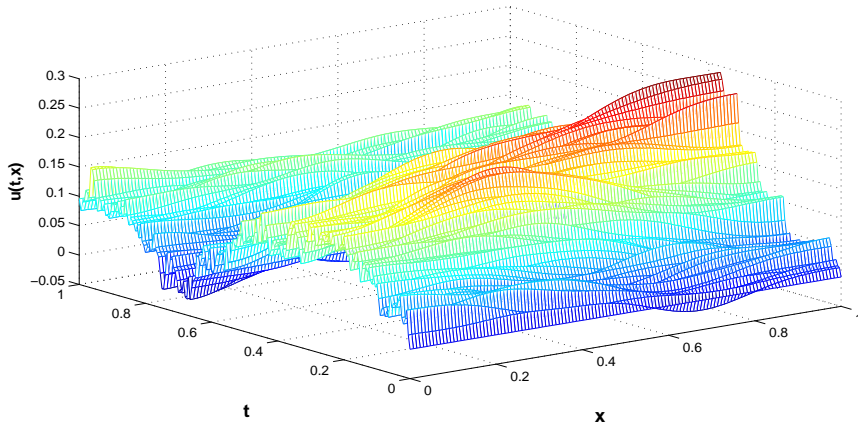


Figure 14: Solution of Burgers equation (5.16), for noise intensities $\sigma = 0.5$ and with $u_0(x)=0$, $N = 128$. Although mean quantities agree, this is very different from boundary forcing. See Figure 15. fig16

We conclude from Theorems 5.1 and 5.2 that the mean energy and averaged mean correlation function for $v(t)$ and $Z(t)$ are the same while they have pathwise completely different behavior. Note that these two parameters are important tools in applied science, which are usually used in order to obtain more information about the stochastic function $v(t)$.

Now to compare the impact of boundary noise and body forcing noise in the Burgers equation we also consider

$$\begin{cases} u_t = u_{xx} - uu_x + W_t, \\ u_x(0, t) = 0 \quad u_x(l, t) = 0, \\ u(x, 0) = u_0(x). \end{cases} \quad (5.16) \quad \text{1.28}$$

Here W_t is a Q -Wiener process with a continuous operator. We plot examples of numerical solutions of (5.16) and (1.1) in Figures 14 and 15. It is obvious that the body noise and boundary forcing noise perform completely different.

In addition we also plot M_u for (1.1) and (5.16) numerically. From Figure 16 it is seen that M_u in both cases performs similarly. fig18

5.1 Numerical Experiment of Convergence

In this part, we consider the pathwise approximation error of the stochastic Burgers equation with Neumann boundary noise by the method given in (2.7) in L^2 . Note that for comparing the solutions with different N pathwise, we first calculate the noise for some large N and then use them for all smaller N . Figure 17 illustrates that, the order of convergence is $\frac{1}{2}$. Obviously these are only four examples, but all of a few hundred calculated examples behave similarly. Note that for the unknown solution, we use a numerical approximation with N sufficiently large. The Matlab code is presented for obtaining one path simulation of the method (2.7) (see Matlab code in Figure 18). Note that, here A

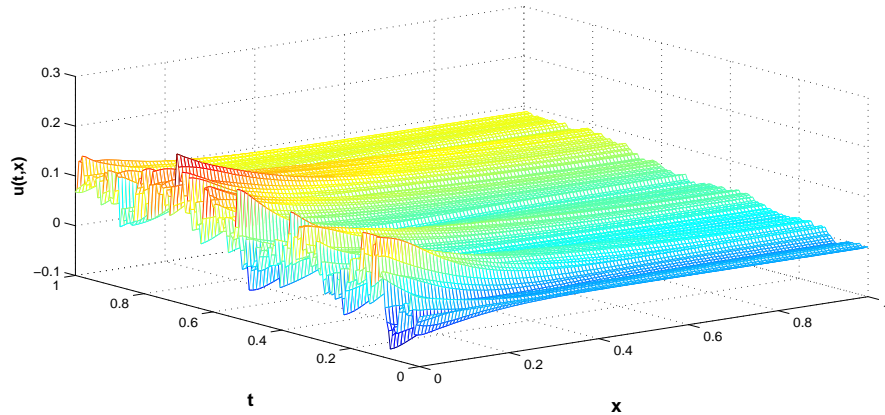


Figure 15: Solution of Burgers equation (1.1) with Neumann boundary noise, for noise intensities $\sigma = 0.5$ and with $u_0(x)=0$, $N = 128$. fig17

is the Laplacian with Neumann boundary condition and thus its eigenpairs are given by $g_k(x) = \sqrt{\frac{2}{l}} \cos\left(\frac{\pi k x}{l}\right)$ and $\lambda_k = -v\left(\frac{k\pi}{l}\right)^2$ for $x \in (0, 1)$, $k \in \mathbb{N}_0$.

For each Fourier mode, we obtain

$$(u_{n,k+1}, g_j)_H = e^{\lambda_j} (u^N, g_j)_H = \sqrt{2} e^{\lambda_j} \int_0^1 u^N(x) \cos(j\pi x) dx \quad (5.17) \quad 1.29$$

for $k = 1, \dots, N - 1$ and therefore we use some numerical integration method (here we choose composite trapezoidal formula) to approximate $(u^N, g_j)_H$. Since the eigenfunctions $g_j(x) = \sqrt{2} \cos(j\pi x)$ are cosine functions, we can invoke built-in functions **fft** in Matlab to perform efficient computations. For this, we defined **dcts** (see Matlab code in Figure 18 lines 20-26) for discrete cosine transform via **fft** in Matlab and **idctc** (see Matlab code in Figure 18 lines 27-34) for composite trapezoidal formula to calculate inner products and **Ddct** (see Matlab code in Figure 18 lines 35-41) to calculate F in (2.7). fig21

6 Conclusion

We have considered the Burgers equation on the interval with boundary Neumann noise on one side, and we obtained series expansion of the stochastic convolution in which each term has the same Brownian motion. Then, a combined application of the Galerkin method and the exponential Euler method has been applied to solve numerically the problem through its mild solution. We have shown that the noise on the boundary grows immediately to the entire domain. Also one can see that as σ is increased, the noise impact on the entire domain is also increased. Then we have analyzed and illustrated some properties of the stochastic term and also shown numerically that the order of convergence is $\frac{1}{2}$, see Figure 17. fig20

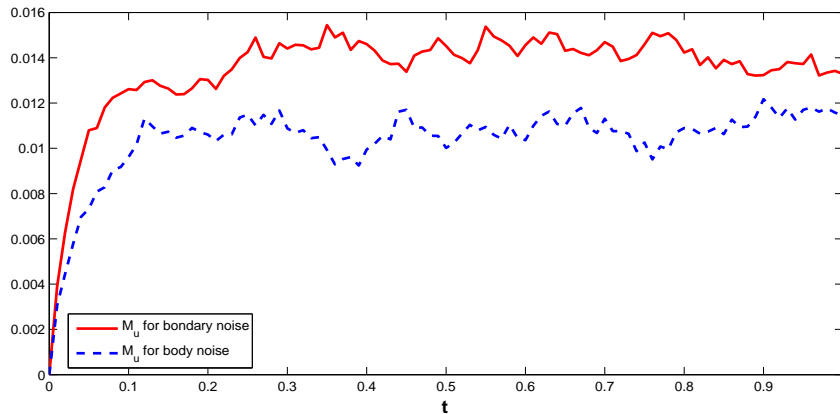


Figure 16: M_u for the Burgers equation (5.16) with body noise and the Burgers equation (1.1) with random Neumann boundary noise, with respect to time, for $\sigma = 0.5$ and $u_0(x) = 0$, $N = 128$.

fig18

References

- [1] A. Alabert, I. Gyöngy, On numerical approximation of stochastic Burgers' equation, From stochastic calculus to mathematical finance, Springer, Berlin, 2006, pp.1–15.
- [2] S. Peszat, J. Zabczyk, Stochastic Partial Differential Equations with Lévy Noise, Cambridge University Press, Cambridge, U.K., 2007. pp. 241–249.
- [3] E. Hausenblas, Numerical analysis of semilinear stochastic evolution equations in Banach spaces , *J. Comput. Appl. Math.*, 147 (2002), 485–516.
- [4] G. Da Prato, J. Zabczyk, Ergodicity for infinite-dimensional systems, vol.229 of London Mathematical Society Lecture Note Series. Cambridge University Press, Cambridge, 1996.
- [5] I. Gyöngy, D. Nualart, On the stochastic Burgers equation in the real line, *Ann. Probab.* 27, 2 (1999), 782–802.
- [6] D. Blömker, J. Duan, Predictability of the Burgers dynamics under model uncertainty. pp. 71–90 in *Stochastic differential equations: Theory and applications. A Volume in Honor of Professor Boris L Rozovskii* (Ed. P. Baxendale, S. Lototsky), 2007.
- [7] A. Jentzen and P.E. Kloeden, Overcoming the order barrier in the numerical approximation of stochastic partial differential equations with additive space-time noise , *Proc. Roy. Soc. London Ser A.*, 465 (2009), No. 2102, 649-667.
- [8] A. Jentzen, P.E. Kloeden, and G. Winkel, Efficient simulation of non- linear parabolic SPDEs with additive noise , *Ann. Appl. Probab.*, 21 (2011), 908-950.
- [9] A. Jentzen, Taylor Expansions for Stochastic Partial Differential Equations. Johann Wolfgang Goethe-University, Frankfurt am Main, Germany, 2009. Dissertation.

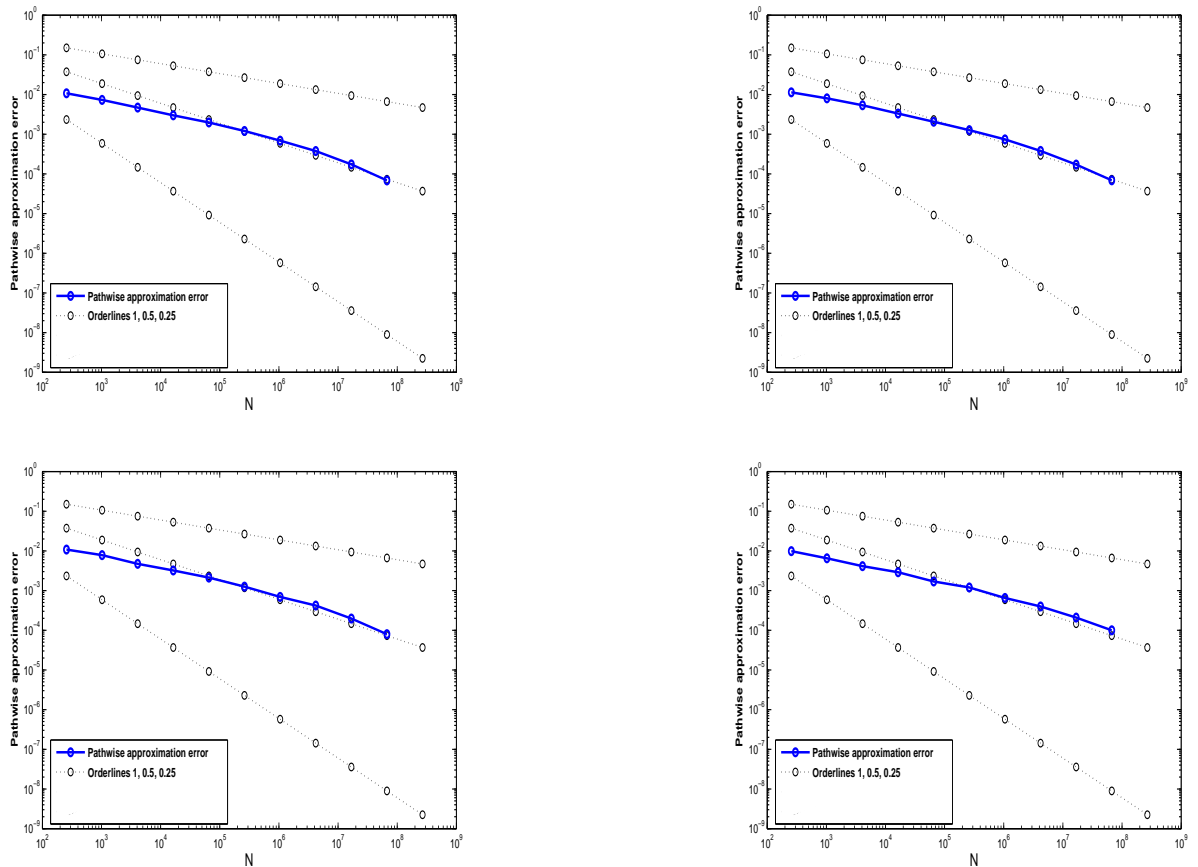


Figure 17: Pathwise approximation error against N for $N \in \{16, 32, \dots, 8192\}$ for four random $\omega \in \Omega$. These are only four examples, but all other calculated trajectories behave similarly.

fig20

- [10] [10] R. Sowers, Multidimensional reaction–diffusion equations with white noise boundary perturbations, *Ann. Probab.* 22 (1994) 2071–2121.
- [11] [11] A. Debussches, J. Printems, Numerical simulation of the stochastic Korteweg-de Vries equation, *Physica D* 134 (2) (1999) 200–226.
- [12] [12] Z. Brzezniak, S. Peszat, Hyperbolic equations with random boundary conditions, *Interdisciplinary Math. Sci.* 8 (2009) 1–21. -
- [13] [13] I. Gyöngy, A. Millet, Rate of convergence of space time approximations for stochastic evolution equations, *Potent. Anal.* (2008).
- [15] [14] C. Prevot, M. Röckner, A concise course on stochastic partial differential equations, vol. 1905 of *Lecture Notes in Mathematics*, Springer, Berlin., 2007.
- [16] [15] J. B. Walsh, On numerical solutions of the stochastic wave equation, *Illinois J. Math.*, 50, 1-4 (2006), 991–1018 (electronic).
- [17] [16] T. Shardlow, Numerical methods for stochastic parabolic PDEs, *Numer. Funct. Anal. Optim.*, 20, 1-2 (1999), 121–145

- [18] [17] I. Gyöngy, N. Krylov, An accelerated splitting-up method for parabolic equations , *SIAM J. Math. Anal.* , 37, 4 (2005), 1070–1097 (electronic).
- [19] [18] I. Gyöngy, T. Martinez, On numerical solution of stochastic partial differential equations of elliptic type , *Stochastics.*, 78, 4 (2006), 213-231.
- [20] [19] T. Runst, and W. Sickel, sobolev spaces of fractional order, Nemytskij operators, nonlinear partial differential equations, vol. 3 of de Gruyter Series in Nonlinear Analysis and Applications , *Walter de Gruyter Co. Berlin.*,(1996).
- [21] [20] A. V. Balakrishnan, Identification and stochastic control of a class of distributed systems with boundary noise. Control theory, numerical methods and computer systems modelling (Internat. Sympos., IRIA LABORIA, Rocquencourt, 1974), pp. 163–178, Lecture Notes in Econom. and Math. Systems, Vol. 107, Springer, Berlin,1975. , *Walter de Gruyter Co. Berlin.*,(1996).
- [22] [21] A. Pazy, Semigroups of Linear Operators and Applications to Partial Differential Equations, *Springer*, (1992)
- [23] [22] X. Shengqiang, J. Duan, A Taylor expansion approach for solving partial differential equations with random Neumann boundary conditions. , *Applied Mathematics and Computation*, 217 (2011) 95329542.
- [24] [23] D. Blömker, M. Kamrani, S.M. Hosseini, Full discretization of the stochastic Burgers equation with correlated noise , *IMA Journal of Numerical Analysis*, (2013) 1 - 24.

```

0. function onepathsimul()
1. clear all;clc;
2. N = 10; M = 100; SqrM=sqrt(M);      %%% time stepsize 1/M and P_N
3. A=-pi^2*(1:N-1).^2; B=[1/M (1-exp(A/M))./A];
4. C=[1/SqrM sqrt((1-exp(2*A/M))./(-2*A))];
5. Y = [0, sqrt(2)/2, zeros(1,N-2)];%%% initial function
6. for m = 1:M
7. for i=1:N
8. for j=1:N
9. CM(i,j)=coo(i,j);
10. end
11. end
12. CM=chol(CM);
13. y = dctc(Y)*sqrt(2);
14. Dy = -sqrt(2)*pi*Ddst([0:N-1].*Y);
15. Fy = -1*y.*Dy;      %%% function - Y Y' values at grid points
16. noise=1*C.*(CM'*randn(N,1))';
17. Y=exp([0 A]/M).*Y+B.*idctc(Fy)*sqrt(2)+noise;
18. end
19. plot((0:N-1)/(N-1),dctc(Y)*sqrt(2));

20. function Z = dctc(z)      %%% to calculate function values at grid points
21. n=length(z);
22. D=zeros(2*n-2);
23. D(1:n) = z;
24. DD=fft(D);
25. Z = real(DD(1:n));
26. end

27. function z = idctc(Z)    %composite trapezoidal formula to calculate inner
products
28. n=length(Z);
29. if n>2;
30. Z(2:n-1) = 2*Z(2:n-1);
31. end
32. DD=dctc(Z)/(2*(n-1));
33. z = real(DD(1:n));
34. end

35. function DF = Ddst(xx)  %to calculate derivative function Y' values at
grid points
36. n=length(xx);
37. D=zeros(2*n-2);
38. D(1:n) = xx;
39. DD=fft(D);
40. DF = -imag(DD(1:n));
41. end

42. function co=coo(i,j)    % to calculate covariance matrix
43. li=(i*pi)^2;
44. lj=(j*pi)^2;
45. dlt=.01;
46. co=(1-exp(-dlt*(li+lj)))/(li+lj);
47. end
48. end

```

Figure 18: Matlab code to simulate one path by the method ^{11.6}(2.5).

fig21